Inorganic Nanoplates

DOI: 10.1002/ange.200601031

Synthesis, Optical Properties, and Self-Assembly of Ultrathin Hexagonal In_2S_3 Nanoplates**

*Kang Hyun Park, Kwonho Jang, and Seung Uk Son**

Anisotropic nonspherical nanomaterials have attracted a special attention in material science because of their unique chemical, physical, and optical properties, which are greatly affected by their shape and size.[1] Thus, many efforts have been made to synthesize nanorods and nanowires.[2] Compared with one-dimensional (1D) structures, 2D nanomaterials such as nanoplates and nanodisks have been relatively little explored and require further investigation. To date the following nanoplates have been prepared: hexagonal[3] ($Co(OH)_2$, Cu_2S, $SbTe_3$, Bi_2Te_3, etc.), trigonal[4] (Au, Ag, Pd, Bi, Se, LaF_3, etc.), square[5] (rare earth metals, Bi_2WO_6, etc.), and circular[6] (Ag, Co, etc.).

Over the last two decades, the chemical and physical properties of diverse semiconductor nanocrystals have been investigated.[7] Compared to the corresponding conventional bulk materials, semiconductor nanomaterials show unique optical, mechanical, electronic, and catalytic properties which are highly dependent on size and shape. Of the known semiconductor nanomaterials, perhaps the semiconducting metal chalcogenides have been studied most widely. In particular, most studies have focused on II–VI quantum dots (QDs) such as CdS, ZnS, and CdSe.[8] Moreover, I–VI QDs such as Ag_2S and Cu_2S have received significant attention.[9] Compared with the semiconductor nanomaterials mentioned above, the optical and electronic properties of metal chalcogenides which have 1:1.5 molar ratio of metal to chalcogenide in their unit cells have received comparatively little attention. These include In_2S_3, Bi_2S_3, and Sb_2S_3 nanocrystals.[10]

Indium sulfide (In_2S_3) exists in three different crystalline forms: α-In_2S_3 (defect cubic), β-In_2S_3 (defect spinel), and γ-In_2S_3 (layered structure).[11] Of these, β-In_2S_3 is an n-type semiconductor with a band gap of 2.0–2.3 eV and is stable above 420 °C.[12] Moreover, the unique luminescence properties of β-In_2S_3 have enabled its use as a phosphor in display devices.[13] Furthermore, its photoconductive properties[14] make it a promising candidate for photovoltaic applications such as solar cells. Recently, it was reported that solar cell devices prepared by using β-In_2S_3 as a buffer layer show 16.4% conversion efficiency, which is very close to that of the standard CdS buffer layer.[15] Much effort has been made to replace highly toxic cadmium with other metals for environmental reasons.[16]

A number of synthetic methods[17] have been developed to prepare β-In_2S_3, for example, direct reacting of the elements at high temperature, heating In_2O_3 in H_2S, thermal decomposition of organometallic precursors, and metathesis reaction between $InCl_3$ and Li_2S. To fabricate thin films of β-In_2S_3 for solar cell applications, several deposition techniques, such as organometallic chemical deposition, spray pyrolysis, and chemical bath deposition, have been developed.[18] β-In_2S_3 can also be prepared by a wet chemical approach,[19] that is, by reaction between aqueous $InCl_3$ and H_2S, $(NH_4)_2S$, or NaSH; by laser-induced formation of In_2S_3 from sodium polysulfide in aqueous solution; by using red light and Na_2S; by forming colloidal particles in reverse micelles; by injecting H_2S into $In(ClO_4)_3$ solution; by hydrothermal treatment of an acidic sol of $InCl_3$ and Na_2S; or by sonochemical synthesis from $InCl_3$ and $MeCSNH_2$. Recently, 3-nm β-In_2S_3 nanocrystals were prepared by an arrested-precipitation method using aqueous $InCl_3$ solution and a thiol stabilizer.[20] However, as far as we are aware, the synthesis of β-In_2S_3 in organic media

[*] Dr. K. H. Park, K. Jang, Prof. S. U. Son
Department of Chemistry
Sungkyunkwan University
Suwon 440-746 (Korea)
Fax: (+82) 31-299-4572
E-mail: sson@skku.edu

[**] This work was supported by the Korea Research Foundation Grant funded by the Korean Government (MOEHRD, KRF-2005-005J11901) and through a Faculty Research Fund-2005 funded by Sungkyunkwan University. We thank J. S. Ju at Cooperative Center for Research Facilities at Sungkyunkwan University for TEM studies.

Supporting information for this article is available on the WWW under http://www.angewandte.org or from the author.

has received little attention, although it is well recognized that various organic surfactants can be excellent reaction media for synthesis of high-quality nanocrystals.[21]

Herein we report on the synthesis of monodisperse hexagonal β-In_2S_3 nanoplates of 0.76-nm thickness in organic media at high temperature by using the arrested-precipitation method. In a typical synthesis, oleylamine was used as a stabilizer and solvent. Anhydrous $InCl_3$ and sulfur powder were dissolved in well-dried oleylamine (9–18 mL), and the mixture was then heated to 215 °C and held at this temperature for 1 h. A bright yellow precipitate formed during the aging step. The TEM images of these precipitates revealed hexagonal nanoparticles (Figure 1 a–c). More detailled TEM

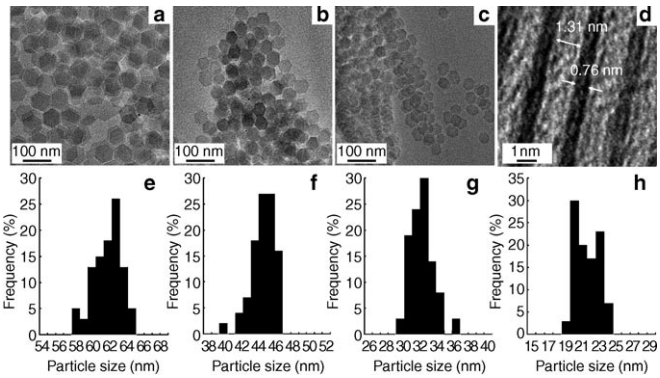

Figure 1. TEM images of a) 63-nm, b) 45-nm, and c) 33-nm β-In_2S_3 nanoplates; d) side view of nanoplates; and histograms illustrating the particle size distributions for e) 63-nm, f) 45-nm, g) 33-nm, and h) 22-nm β-In_2S_3 nanoplates.

investigation showed the synthesized nanoparticles to have a hexagonal plate form. Side views of these plates were obtained on grids, and high-resolution (HR) TEM revealed a plate thickness of 0.76 nm (Figure 1 d), which makes them, as far as we are aware, the thinnest nanoplates known.[22]

Moreover, by changing the concentration of the precursor in oleylamine, we were able to control the size of these hexagonal nanoplates, as shown in Figures 1 a–c and e–h. Using 0.10 M precursor solution, we obtained 63-nm hexagonal nanoplates, and when its concentration was reduced to 0.050 M, the nanoplate size decreased to 45 nm. Also we obtained 33- and 22-nm hexagonal nanoplates using 0.025 M and 0.00125 M precursor solutions, respectively. Interestingly, the nanoplate thickness remained constant throughout the above experiments, and this implies that growth along one plane is much slower than along the others. Unfortunately, numerous trials to determine the retarded-growth direction by HRTEM were unsuccessful because of the extreme thinness of the plates. However, we could get some information about this retarded-growth direction from X-ray diffraction patterns.

Figure 2 shows representative powder X-ray diffraction (XRD) and electron diffraction (ED) patterns of 33-nm hexagonal nanoplates. The powder XRD patterns revealed three sharp peaks at 27.2, 47.9, and 55.8° originating from (109), (400), and (533), which are very close to those reported for β-In_2S_3 (JCPDS card 25-390).[23] From the Debye–Scherrer

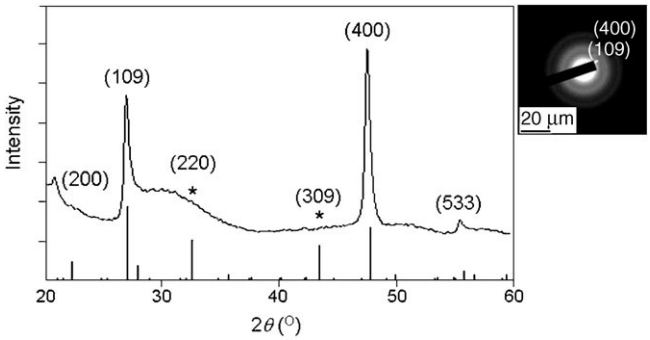

Figure 2. Powder XRD (left) and ED (right) patterns of 33-nm In_2S_3 nanoplates.

equation, the size of the nanoplates was calculated to be 37 nm from the half-width of the (400) diffraction peak, which is consistent with the size determined by TEM. We could not find the (220) and (309) diffraction peaks, which were expected at 32 and 44° correspondingly. According to a library spectrum[23] of bulk β-In_2S_3, the (220) and (309) peaks should be of high intensity. Thus, we suggest that the retarded growth direction may be related to these two lattice planes. The ED pattern shows two broad diffraction circles, which correspond to *d* spacings of 3.10 and 1.94 Å, respectively. These are consistent with the literature values of 3.241 and 1.912 Å originating from the (109) and (400) reflections of β-In_2S_3.[23]

To confirm the chemical stoichiometry of the synthesized nanoplates, we performed energy dispersive spectroscopy (EDS) for indium and sulfur on four samples. All samples showed In:S = 1:1.5 (see Supporting Information for EDS spectra of all samples). Figure 3 shows a representative EDS spectrum of 45-nm nanoplates. It is noteworthy that In_2S_3 remained the sole product when the amount of sulfur was reduced to 0.075 equivalents versus indium.

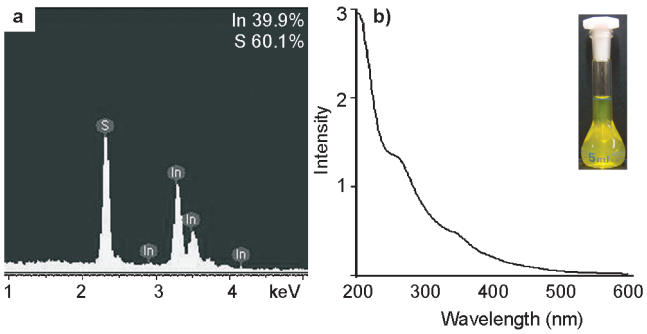

Figure 3. a) EDS and b) UV/Vis absorption spectra of 45-nm In_2S_3 nanoplates, inset: photo of sample.

We carried out UV/Vis absorption and photoluminescence (PL) studies to investigate the optical properties of the ultrathin hexagonal nanoplates. Dispersed hexane solutions of nanoplates had a slightly luminescent yellow color (inset in Figure 3 b). Figure 3 b shows a representative UV/Vis absorption spectrum of 45-nm hexagonal nanoplates. Compared to the absorption peak of 3.0-nm nanoparticles,[20] that of 45-nm

nanoplates was red-shifted by 30 nm. In addition, the UV/Vis spectra of nanoplates showed a steplike shape, which was mentioned to be an indicator of conduction and valence band transition in β-In_2S_3.[20] Interestingly, we observed no significant differences between the UV/Vis spectra of 63-, 45-, 33-, and 22-nm nanoplates (see Supporting Information for UV/Vis spectra of 63-, 45-, and 22-nm nanoplates), which implies that the sizes (22–63 nm) of the nanoplates are beyond the quantum confinement range. Detailed optical characterizations including emission, quantum yields, and decay kinetics will be reported elsewhere. In addition, the electroluminescence properties of nanoplates will be characterized after layering on indium tin oxide (ITO)/glass by the Langmuir–Blodgett technique.

For applications in various optical devices, including solar cells, thin-film fabrication techniques are needed.[18] Since the hexagonal nanoplates are extremely thin, we believe that these nanomaterials can be used as building blocks to prepare subnanometer films by self-assembly. The high surface area of the 2D nanoplates, as compared with 0D or 1D nanomaterials, is interesting from the aspect of self-assembly behavior. Recently, the formation of spherelike macrostructures by self-assembly of hexagonal nanoplates was reported.[24]

Hexagonal In_2S_3 nanoplates showed two self-assembly patterns in TEM studies: parallel alignment to a solid support and upright alignment due to interactions with other nanoplates. Interestingly, these self-assembly behaviors depend on nanoplate size and concentration. When nanoplate size was reduced from 63 to 22 nm, upright alignment was favored, and when the concentration of nanoplates in the mother solution was reduced, parallel alignment was favorable, as sketched in Figure 4.

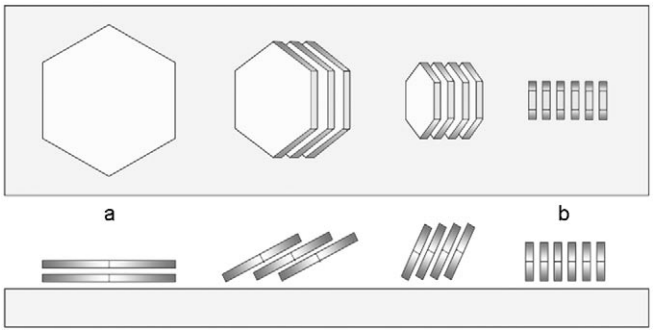

Figure 4. Sketch of size-dependent self-assembly of In_2S_3 nanoplates. a) Parallel alignment and b) upright alignment.

The 63-nm nanoplates showed a preference toward parallel alignment to a solid support (Figure 5a), and we also observed a regular parallel packing structure (Figure 5b). For 45-nm nanoplates, the self-assembly process was strongly concentration dependent. When we used a dilute solution (ca. 5 mg of nanoplates in 2 mL of dichloromethane) to induce self-assembly by drop casting on a grid, we observed substantial parallel alignment to the solid support (Figure 5c). In some regions of the grid, we observed both parallel and upright alignments of 45-nm nanoplates (Figure 5d). When we used a relatively concentrated sample of 45-nm nanoplates

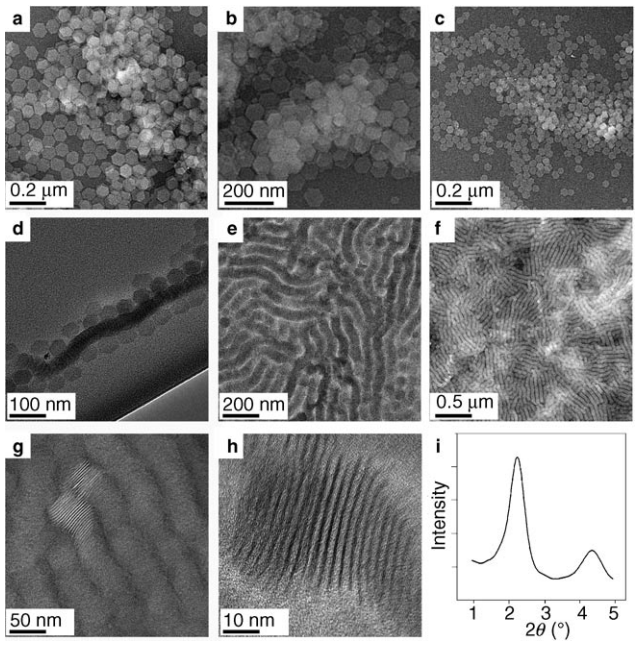

Figure 5. TEM images of a, b) parallel-aligned 63-nm nanoplates, c–f) 45-nm nanoplates at relatively low (c, d) and high (e, f) concentration, and g, h) 33-nm nanoplates at relatively high concentration; i) low-angle powder XRD pattern of self-assembled 45-nm nanoplates.

(ca. 20 mg in 1 mL of dichloromethane), we observed upright alignment in almost all regions (Figure 5e, f. In the case of 33- and 22-nm nanoplates, the upright alignment was strongly favored. It can be speculated that this behavior is due to greater attraction between larger nanoplates and the carbon film on the grid. Interestingly, more hexagonal nanoplates which are perpendicular to the surface of the grid (parallel to electron beam of the TEM) were observed for 33- and 22-nm nanoplates. (Figure 5g, h) Using HRTEM, we measured the thicknesses of and the distances between aligned nanoplates. The inside distance between two aligned nanoplates was about 1.3 nm and nanoplate thickness was 0.76 nm. (Figure 1d) Low-angle powder XRD studies also provided information about distances in the self-assembled structures. The two peaks in the low-angle XRD pattern in Figure 5i correspond to 2.7 and 1.3 nm, which agree well with the results of HRTEM studies. This understanding of the self-assembly behavior of nanoplates could be helpful for future applications of these materials to photovoltaic devices.

In conclusion, we have synthesized ultrathin hexagonal β-In_2S_3 nanoplates of unprecedented thinness by an arrested-precipitation method from organic media and characterized them using TEM, powder XRD, and EDS studies. These nanoplates showed intriguing optical properties and self-assembly behavior. β-In_2S_3 is a common material for solar cell applications,[18] and many efforts have been made to fabricate this material in thin-film form on a suitable support. The β-In_2S_3 nanoplates are 0.76 nm thick and show size- and concentration-dependent self-assembly behavior. We are now trying to assemble a monolayer on a solid support such as ITO. We believe that these self-assembling nanoplates can

be used for the development of diverse ultrathin nanodevices,[25] such as solar cells.

Experimental Section

All spectroscopic studies were performed on as-prepared nanoplates without employing any size-selection process. TEM and HRTEM images were recorded with a JEOL 2100F unit operated at 200 kV. The self-assembly of nanoplates was carried out on carbon-coated copper grids by drop casting nanoplates dispersed in dichloromethane. EDS was preformed on a FE-SEM (JSM6700F). Powder XRD patterns were obtained on a Rigaku MAX-2200 with filtered $Cu_{K\alpha}$ radiation. UV/Vis absorption spectra of hexagonal nanoplates were recorded on a Jasco V-500 spectrophotometer. For UV/Vis experiments, solutions of 4 mg of nanoplates in hexane (HPLC grade, Burdick & Jackson, 100 mL) were used.

In a typical synthetic procedure, anhydrous $InCl_3$ and 1.5 equivalents of sulfur powder were added to 9–18 mL of oleylamine. After heating the mixture at 110 °C for 1 h, the temperature was increased to 215 °C and held for 1 h. After cooling the solution to 35 °C, methanol was added to the reaction mixture and the precipitate formed was retrieved by centrifugation. After repeating this washing procedure twice, the obtained precipitates were dried under vacuum. Using 0.10, 0.050, 0.025, 0.0125 M solutions of indium chloride in oleylamine, we obtained 63-, 45-, 33-, and 22-nm hexagonal nanoplates.

Received: March 15, 2006
Published online: June 22, 2006

Keywords: indium · nanostructures · self-assembly · semiconductors · sulfur

[1] Selected literature: a) J. T. Hu, T. W. Odom, C. M. Lieber, *Acc. Chem. Res.* **1999**, *32*, 435; b) Y. Sun, Y. Xia, *Science* **2002**, *298*, 2176; c) B. Nikoobakht, M. A. El-Sayed, *Chem. Mater.* **2003**, *15*, 1957; d) special issue on nanowires: *Adv. Mater.* **2003**, *15*, 351–466.

[2] a) Y. Cui, C. M. Lieber, *Science* **2001**, *291*, 851; b) M. Huang, S. Mao, H. Feick, H. Yan, Y. Wu, H. Kind, E. Weber, R. Russo, P. Yang, *Science* **2001**, *292*, 1897; c) T. Hanrath, B. A. Korgel, *J. Am. Chem. Soc.* **2002**, *124*, 1424; d) F. Dumestre, B. Chaudret, C. Amiens, M.-C. Fromen, M.-J. Casanove, M. Respaud, P. Zurcher, *Angew. Chem.* **2002**, *114*, 4462; *Angew. Chem. Int. Ed.* **2002**, *41*, 4286; e) W. U. Huynh, J. J. Dittmer, A. P. Alivisatos, *Science* **2002**, *295*, 2425; f) C. Qian, F. Kim, L. Ma, F. Tsui, P. Yang, J. Liu, *J. Am. Chem. Soc.* **2004**, *126*, 1195.

[3] a) M. B. Sigman, Jr., A. Ghezelbash, T. Hanrath, A. E. Sanuders, F. Lee, B. A. Korgel, *J. Am. Chem. Soc.* **2003**, *125*, 16050; b) H.-T. Zhang, G. Wu, X.-H. Chen, *Langmuir* **2005**, *21*, 4281; c) W. Wang, B. Poudel, J. Yang, D. Z. Wang, Z. F. Ren, *J. Am. Chem. Soc.* **2005**, *127*, 13792; d) Y. Hou, H. Kondoh, M. Shimojo, T. Kogure, T. Ohta, *J. Phys. Chem. B* **2005**, *109*, 19094; e) W. Lu, Y. Ding, Y. Chen, Z. L. Wang, J. Fang, *J. Am. Chem. Soc.* **2005**, *127*, 10112; f) S. S. Garje, D. J. Eisler, J. S. Ritch, M. Afzaal, P. O'Brien, T. Chivers, *J. Am. Chem. Soc.* **2006**, *128*, 3120.

[4] a) S. Chen, D. L. Carroll, *J. Phys. Chem. B* **2004**, *108*, 5500; b) Y.-W. Zhang, X. Sun, R. Si, L. -P, You, C.-H. Yan, *J. Am. Chem. Soc.* **2005**, *127*, 3260; c) Y. He, G. Shi, *J. Phys. Chem. B* **2005**, *109*, 17503; d) Y. Xiong, J. M. McLellan, J. Chen, Y. Yin, Z.-Y. Li, Y. Xia, *J. Am. Chem. Soc.* **2005**, *127*, 17118; e) K. Aslan, J. R. Lakowicz, C. D. Geddes, *J. Phys. Chem. B* **2005**, *109*, 6247; f) B. Liu, J. Xie, J. Y. Lee, Y. P. Ting, J. P. Chen, *J. Phys. Chem. B* **2005**, *109*, 15256.

[5] a) Y. C. Cao, *J. Am. Chem. Soc.* **2004**, *126*, 7456; b) R. Si, Ya.-W. Zhang, L.-P. You, C.-H. Yan, *Angew. Chem.* **2005**, *117*, 3320; *Angew. Chem. Int. Ed.* **2005**, *44*, 3256; c) T. Yu, J. Joo, Y. I. Park, T. Hyeon, *J. Am. Chem. Soc.* **2006**, *128*, 1786.

[6] a) V. F. Puntes, K. M. Krishnan, A. P. Alivisatos, *Science* **2001**, *291*, 2115; b) V. F. Puntes, D. Zanchet, C. K. Erdonmez, A. P. Alivisatos, *J. Am. Chem. Soc.* **2002**, *124*, 12874; c) S. Chen, Z. Fan, D. L. Carroll, *J. Phys. Chem. B* **2002**, *106*, 10777.

[7] a) H. Weller, *Angew. Chem.* **1993**, *105*, 43; *Angew. Chem. Int. Ed. Engl.* **1993**, *32*, 41; b) A. P. Alivisatos, *J. Phys. Chem.* **1996**, *100*, 13226; c) S. Empedocles, M. Bawendi, *Acc. Chem. Res.* **1999**, *32*, 389; d) M. Nirmal, L. Brus, *Acc. Chem. Res.* **1999**, *32*, 407; e) Z. A. Peng, X. Peng, *J. Am. Chem. Soc.* **2002**, *124*, 3343; f) D. J. Milliron, S. M. Hughes, Y. Cui, L. Manna, J. Li, L.-W. Wang, A. P. Alivisatos, *Nature* **2004**, *430*, 190.

[8] Selected examples: a) Z. A. Peng, X. Peng, *J. Am. Chem. Soc.* **2001**, *123*, 183; b) Y.-W. Jun, S.-M. Lee, N.-J. Kang, J. Cheon, *J. Am. Chem. Soc.* **2001**, *123*, 5150; c) J. Joo, H. B. Na, T. Yu, J. H. Yu, Y. W. Kim, F. Wu, J. Z. Zhang. T. Hyeon, *J. Am. Chem. Soc.* **2003**, *125*, 11100; d) Y. C. Cao, J. Wang, *J. Am. Chem. Soc.* **2004**, *126*, 14336.

[9] a) L. Motte, M. P. Pileni, *J. Phys. Chem. B* **1998**, *102*, 4104; b) X. Wen, W. Zhang, S. Yang, Z. R. Dai, Z. L. Wang, *Nano Lett.* **2002**, *2*, 1397; c) L. Chen, Y.-B. Chen, L.-M. Wu, *J. Am. Chem. Soc.* **2004**, *126*, 16334; d) Z. Liu, D. Xu, J. Liang, J. Shen, S. Zhang, Y. Quan, *J. Phys. Chem. B* **2005**, *109*, 10699.

[10] a) N. M. Dimitrijevic, P. V. Kamat, *Langmuir* **1987**, *3*, 1004; b) R. Vogel, P. Hoyer, H. Weller, *J. Phys. Chem.* **1994**, *98*, 3183; c) R. Suarez, P. K. Nair, P. V. Kamat, *Langmuir* **1998**, *14*, 3236.

[11] a) R. Diehl, R. Nitsche, *J. Cryst. Growth* **1975**, *28*, 306; b) S.-H. Yu, L. Shu, Y.-S. Wu, J. Yang, Y. Xie, Y.-T. Qian, *J. Am. Ceram. Soc.* **1999**, *82*, 457.

[12] T. Asikainen, M. Ritala, M. Leskela, *Appl. Surf. Sci.* **1994**, *82*/83, 122.

[13] a) Japanese patent application, *Chem. Abstr.* **1981**, *95*, 107324x; b) S. Yu, L. Shu, Y. Qian, Y. Xie, J. Yang, L. Yang, *Mater. Res. Bull.* **1998**, *33*, 717.

[14] a) W.-T. Kim, C.-D. Kim, *J. Appl. Phys.* **1986**, *60*, 2631; b) R. Nomura, S. Inazawa, K. Kanaya, H. Matsuda, *Appl. Organomet. Chem.* **1989**, *3*, 195.

[15] a) E. Dalas, S. Sakkopoulos, E. Vitoratos, G. Maroulis, L. Kobotiatis, *J. Mater. Sci.* **1993**, *28*, 5456; b) N. Naghavi, S, Spiering, M. Powalla, B. Cavana, D. Lincot, *Prog. Photovoltaics Res. Appl.* **2003**, *11*, 437; c) J. Sterner, J. Malmstrom, L. Stolt, *Prog. Photovoltaics Res. Appl.* **2005**, *13*, 179.

[16] a) D. Braunger, D. Hariskos, T. Walter, H. W. Schock, *Solar Energy Mater. Solar Cells* **1996**, *40*, 97; b) A. Ennaoui, C. D. Lokhande, M. Weber, R. Scheer, H. J. Lawerenz, *14th European Photovoltaic Solar Energy Conference (EPSEC)*, Barcelona, **1997**.

[17] a) H. B. Richard, H. M. William, *J. Phys. Chem. Solids* **1959**, *10*, 333; b) C. Kaito, Y. Saito, K. Fujita, *J. Cryst. Growth* **1989**, *94*, 967; c) J. C. Fitzmaurice, I. P. Parkin, *Main Group Met. Chem.* **1994**, *17*, 481.

[18] a) R. Nomura, K. Konishi, H. Matsuda, *Thin Solid Films* **1991**, *198*, 339; b) C. D. Lokhande, A. Ennaoui, P. S. Patil, M. Giersig, K. Diesner, M. Muller, H. Tributsch, *Thin Solid Films* **1999**, *340*, 18.

[19] a) P. N. Kumta, P. P. Phule, S. H. Risbud, *Mater. Lett.* **1987**, *5*, 401; b) P. V. Kamat, N. M. Dimitrijevic, R. W. Fessenden, *J. Phys. Chem.* **1988**, *92*, 2324; c) Y. Nosaka, N. Ohta, H. Miyama, *J. Phys. Chem.* **1990**, *94*, 3752; d) S. Avivi, O. Palchik, W. Palchick, M. A. Slifkin, A. M. Weiss, A. Gedanken, *Chem. Mater.* **2001**, *13*, 2195.

[20] D. K. Nagesha, X. Liang, A. A. Mamedov, G. Gainer, M. A. Eastman, M. Giersig, J.-J. Song, T. Ni, N. A. Kotov, *J. Phys. Chem. B* **2001**, *105*, 7490.

[21] a) S. U. Son, Y. Jang, J. Park, H. B. Na, H. M. Park, H. J. Yun, J. Lee, T. Hyeon, *J. Am. Chem. Soc.* **2004**, *126*, 5026; b) S. U. Son, U. K. Park, J. Park, T. Hyeon, *Chem. Commun.* **2004**, 778;

c) S. U. Son, Y. Jang, K. Y. Yoon, C. An. Y. Hwang, J.-G. Park, H.-J. Noh, J.-Y. Kim, J.-H. Park, T. Hyeon, *Chem. Commun.* **2005**, 86.
[22] For β-In_2S_3, the parameters of the tetragonal crystal lattice are $a = b = 7.62$ Å, $c = 32.32$ Å.
[23] Powder Diffraction File Sets 1 – 5 (Revised), Joint Committee on Powder Diffraction Standards, Philadelphia, **1967**, pp. 5-0729–5-0731.
[24] Z. R. Tian, J. A. Voigt, J. Liu, B. Mckenzie, M. J. Mcdermott, M. A. Rodriguez, H. Konishi, H. Xu, *Nat. Mater.* **2003**, *2*, 821.
[25] *Physics of Quantum Well Devices* (Ed.: B. R. Nag), Kluwer, Dordrecht, **2000**.

